

How to emulate quantum spin liquids and build topological qubits with available quantum hardware

Claudio Chamon,^{1,*} Dmitry Green,^{2,†} and Zhi-Cheng Yang^{1,‡}

¹*Physics Department, Boston University, Boston, MA, 02215, USA*

²*AppliedTQC.com, ResearchPULSE LLC, New York, NY 10065, USA*

(Dated: April 8, 2022)

We show how to construct fully quantum multi-spin interactions using only two-body Ising interactions plus a uniform transverse field. We then provide an explicit embedding of simple gauge models, such as the surface code, into the D-Wave chimera architecture. Taken as whole this is a way to build topological qubits using existing hardware. The scheme is generalizable to other gauge-like theories, for example those with fractonic topological order such as the X-cube model. The bottom-up construction of this paper is a blueprint to emulate topologically ordered quantum spin liquids in programmable quantum machines.

Introduction – In the quest for quantum computing, quantum annealers (QA) are widely considered to be the least promising candidates. A leading technology company offered the following snippet on its website. We reproduce this quote not to single out any of the tremendous research efforts, but because it is a succinct summary of the conventional view:

The quantum annealer is least powerful and most restrictive form of quantum computers. It is the easiest to build, yet can only perform one specific function. The consensus of the scientific community is that a quantum annealer has no known advantages over conventional computing. [1]

On the other end of the complexity spectrum is topological quantum computing (TQC). Since the original proposal by Kitaev [2], a large body of detailed proposals for its implementation have been put forward [3–5]. However, building even a single topological qubit has proven to be daunting [6].

QA systems, on the other hand, have thousands of qubits already available (e.g., the commercially available D-Wave machines [7]). The tradeoff is that QA qubits are not easily manipulable via quantum gates, rather their main use is for large optimization problems, which is the “specific function” of the quote above.

But what if the large number of QA qubits, as “restrictive” as they are, were wired to have topological entanglement? Can that be done? If we can use the simple QA qubits to assemble topological qubits, then being the “easiest to build” becomes their greatest strength. We show in this paper that a standard QA architecture can in fact be programmed to reproduce topologically entangled states by configuring interactions within small clusters of spins.

Our prescription has implications to two important current thrusts: quantum computing and quantum materials. Firstly, we prove that in principle one can build effective topological qubits within scalable hardware that is available today. Secondly, we offer a direct route to realizing quantum spin liquids in programmable quantum hardware. Several recent works explored QA to emulate “artificial materials” [8, 9], but the exotic quantum spin liquids were not within reach. Within both contexts, our results highlight that a QA can be made to function as an emulator of topological states (ETS).

Our blueprint can in principle be implemented in any system that supports, at a minimum, a transverse field Ising model with programmable two-spin interactions. We focus on the D-Wave architecture, constructed with superconducting qubits, only because it is, at the time of this writing, the most scalable.

Our basic result is an analytical prescription to implement the quantum \mathbb{Z}_2 gauge theory exactly. This theory was introduced almost 50 years ago [10, 11], and is the grandfather of the toric code [2]. We present an embedding into D-Wave 2000Q which effectively converts its 2048 basic qubits into 256 gauge spins.

We also illustrate how the approach can be used to build more complex models, such as the 3D version of the toric code and the X-cube model. (Note that the above examples are characterized by Abelian statistics. However, a path to non-Abelian excitations may be possible by introducing twists in the underlying lattice [12–14].)

The core of our approach is to generate multi-spin interactions that are hallmarks of lattice gauge theories from which topological entanglement follows. Realizing these interactions has been a major stumbling block in implementing surface codes. There are several proposals in the literature to craft multi-spin interactions. These proposals fall into two categories: those that apply only to the classical limit and break down in the presence of finite transverse field [15–22]; or those that are quantum but abstract, utilizing complex quantum interactions beyond the simple and available ZZ or Ising interaction [23–27]. Our approach is both fully quantum and fits today’s hardware.

* chamon@bu.edu; These authors contributed equally

† dmitry.green@aya.yale.edu; These authors contributed equally

‡ yangzc@bu.edu

Exact construction of the \mathbb{Z}_2 gauge theory and toric code – We begin with a single site plus its links, and then glue these “molecules” together into a full lattice. We proceed in three steps: first we generate a four-spin interaction on the single star; second we highlight a limit of large couplings in which the Hamiltonian of the full lattice is exactly that of the \mathbb{Z}_2 gauge theory; and third we provide numerical evidence that at intermediate couplings, i.e., away from the exact asymptotic limit, our construction stabilizes the spin liquid state. The construction is made possible by a “combinatorial symmetry” that we introduce below.

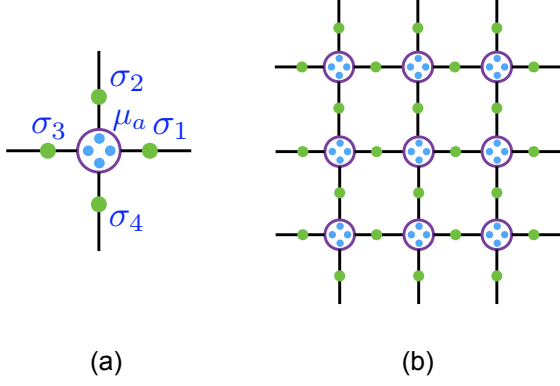


FIG. 1. (a) A single site (star) of the \mathbb{Z}_2 gauge theory/toric code, with 4 matter spins μ_a on the site, and 4 gauge spins σ_i on the links. (b) The full lattice.

• *Exact four-body interaction of a single star* – Consider a site or star, where we define 4 “matter” spins on the site and 4 “gauge” spins on the links, as depicted in Fig. 1. The Hamiltonian for this “molecule” is

$$H = -J \sum_{a=1}^4 \left(\sum_{i=1}^4 W_{ai} \sigma_i^z \right) \mu_a^z - \Gamma \sum_{a=1}^4 \mu_a^x, \quad (1)$$

where the matrix elements $W_{ai} = \pm 1$ encode that all two-spin (ZZ) couplings have the same magnitude J but can be either ferromagnetic (+1) or anti-ferromagnetic (−1). The matter spins μ_a only couple to the gauge spins but not to one another (or other lattice sites). If we freeze for the moment a given z -basis configuration of the gauge spins $\sigma_i^z, i = 1, 2, 3, 4$ (i.e., the transverse field on the gauge spins is off for now), the Hamiltonian for each matter spin μ_a within the molecule is that of a single spin in a magnetic field, whose eigenvalues are

$$E_a^{(\pm)}(\sigma_1^z, \sigma_2^z, \sigma_3^z, \sigma_4^z) = \pm \left[J^2 \left(\sum_{i=1}^4 W_{ai} \sigma_i^z \right)^2 + \Gamma^2 \right]^{1/2}, \quad (2)$$

for each of $a = 1, 2, 3, 4$. We assign a degree of freedom $\tau_a = \pm 1$ that labels the sign of each eigenvalue. The total

energy for a given choice of τ_a is thus $\sum_{a=1}^4 E_a^{(\tau_a)}$. The lowest energy is the case where all $\tau_a = -1$:

$$H_{\tau=-1} = \sum_{a=1}^4 E_a^{(-)}, \quad (3)$$

which is separated from the next level, where at least one τ_a is positive, by a gap of size at least $2|\Gamma|$.

The expression in Eq. (2) can be written, for any value of Γ and J , as

$$E_a^{(\pm)} = \pm C_0 \pm C_2 \sum_{i \neq j}^4 W_{ai} W_{aj} \sigma_i^z \sigma_j^z \pm C_4 W_{a1} W_{a2} W_{a3} W_{a4} \sigma_1^z \sigma_2^z \sigma_3^z \sigma_4^z, \quad (4)$$

which follows from $(\sigma_i^z)^2 = 1$ and $(W_{ai})^2 = 1$. C_0, C_2 and C_4 are constants that depend on J and Γ . Another way to see that this expression is an identity is to expand the square root in Eq. (2) in powers of the σ_i^z ; the binary polynomial inside the square root terminates and the only terms that remain are of the form in Eq. (4).

In order to eliminate the two-spin interactions in the lowest energy sector while retaining the four-spin term, we choose the matrix W_{aj} so as to satisfy: 1) $\sum_{a=1}^4 W_{ai} W_{aj} \propto \delta_{ij}$, or equivalently, $W^\top W \propto \mathbb{1}$; and 2) $\sum_{a=1}^4 W_{a1} W_{a2} W_{a3} W_{a4} \neq 0$.

Matrices with elements ± 1 that satisfy condition 1) are called Hadamard matrices. They maximize the determinant of the information matrix $W^\top W$. Any 4×4 Hadamard matrix satisfies constraint 2) as well, for example:

$$W = \begin{pmatrix} -1 & +1 & +1 & +1 \\ +1 & -1 & +1 & +1 \\ +1 & +1 & -1 & +1 \\ +1 & +1 & +1 & -1 \end{pmatrix}. \quad (5)$$

There are other solutions for W , however they are all equivalent by symmetry. For example, permuting the matter spins or multiplying any row of W by -1 will not affect the spectrum. We pick an intuitive form of W , where the coupling between σ_i^z and μ_a^z is anti-ferromagnetic when $i = a$ and ferromagnetic otherwise.

We thus arrive at the following simple Hamiltonian for the sector with all negative τ 's:

$$H_{\tau=-1} = \gamma - \lambda \sigma_1^z \sigma_2^z \sigma_3^z \sigma_4^z, \quad (6)$$

where the coefficients γ and λ are functions of Γ and J :

$$\begin{aligned} \gamma &= -\frac{1}{2} \left(\sqrt{\Gamma^2 + 16J^2} + 3|\Gamma| + 4\sqrt{\Gamma^2 + 4J^2} \right) \\ \lambda &= -\frac{1}{2} \left(\sqrt{\Gamma^2 + 16J^2} + 3|\Gamma| - 4\sqrt{\Gamma^2 + 4J^2} \right). \end{aligned} \quad (7)$$

These relations follow from the consistency between Eqs. (2) and (4). The parity $P \equiv \sigma_1^z \sigma_2^z \sigma_3^z \sigma_4^z$ for the ground state of Eq. (6) is $P = +1$, since $\lambda > 0$. By modifying the matrix W , we could flip the sign of λ and have

instead the $P = -1$ parity sector as the ground state (for example, by flipping the sign of any one column of W).

- *Limits* – There is an asymptotic limit in which the effective Hamiltonian is *exactly* $H_{\tau=-1}$. This limit corresponds to taking $|\Gamma| \rightarrow \infty$ while keeping λ fixed, which opens an infinite gap to the excited sectors, where at least one $\tau_a = +1$. The splitting $2|\lambda|$ between the two parity states within the lowest energy sector remains finite. The expansion of Eq. (7) in the regime of $J \ll \Gamma$ yields $\lambda = 12J^4/\Gamma^3 + \mathcal{O}(J^6/\Gamma^5)$. (Note that terms of order Γ vanish.) To access this regime we would fix λ and tune J such that

$$J = |\lambda \Gamma^3 / 12|^{1/4}. \quad (8)$$

Physically, in this limit the matter fields μ are extremely massive, and therefore, we can integrate them out to obtain the four-spin effective Hamiltonian.

The opposite (classical Ising) limit where J is large compared to Γ does not work for our purposes. In this limit, the gap to the excited sector with one $\tau_a = +1$ scales as $4J$. However, the splitting $2|\lambda|$ between the two parity states also scales as $4J$. The limit $J \rightarrow \infty$ cannot isolate the ground state sector. Therefore, the correct starting point is the limit of a large transverse field $\Gamma \gg J$.

- *Placing stars in the lattice* – Let us now place the stars in the full lattice, as shown in Fig. 1(b). The full lattice Hamiltonian includes a transverse field $\tilde{\Gamma}$ acting on the gauge spins σ . (When we embed the surface code on the D-Wave machine, the effective $\tilde{\Gamma}$ acting on the gauge spins will in general be smaller than Γ acting on the matter spins, as a result of requiring multiple redundant copies of gauge spins.) This full lattice Hamiltonian is given by

$$H = - \sum_s \left[J \sum_{\substack{a \in s \\ i \in s}} W_{ai} \sigma_i^z \mu_a^z + \Gamma \sum_{a \in s} \mu_a^x \right] - \tilde{\Gamma} \sum_i \sigma_i^x, \quad (9)$$

where the s are stars on the lattice. In the asymptotic limit of large Γ , the low energy $\tau = -1$ sector is given by

$$H_{\tau=-1} = -\lambda \sum_s \prod_{i \in s} \sigma_i^z - \tilde{\Gamma} \sum_i \sigma_i^x. \quad (10)$$

This Hamiltonian is exactly that of the \mathbb{Z}_2 quantum gauge theory, which supports a topological phase for $\tilde{\Gamma}/\lambda$ below a threshold. To get the toric/surface code limit, one only has to notice that the lowest order term that survives in a perturbation theory in $\tilde{\Gamma}/\lambda$ is the term that flips all spins around a plaquette [28–30].

- *Combinatorial symmetry* – The symmetries of our gauge-matter interactions ensure that the correspondence to the desired effective Hamiltonian remains for a wide range of parameters, not simply the asymptotic limit of large Γ . A key feature of the gauge-matter interaction in Eq. (1) is that the *whole spectrum*, not only

the ground state, depends only on the parity P . The energy levels of the 8 states with parity $P = +1$ and 8 states with parity $P = -1$ are explicitly listed in the Supplementary Material, Sec. A. Recall that for a given configuration of gauge spins, there are 16 allowed combinations of $\tau_a = \pm 1$ so this is a non-trivial feature. We refer to this spectral property as *combinatorial symmetry*. A true spin liquid state does not favor any ordered configuration, and this combinatorial symmetry is essential to suppressing all interactions that favor any local ordering on the lattice.

- *Numerical tests* – We shall now provide strong numerical evidence that the projection down to the sector where all τ 's are negative is justified for a wide range of parameters $(\tilde{\Gamma}, \Gamma, J)$. Below we study the spectrum of clusters containing either a single star in the presence of $\tilde{\Gamma}$ or a single plaquette surrounded by a fixed background (with additional details presented in the Supplementary Material, Sec. B). The analysis passes each of the following three tests in favor of a spin liquid *within machine precision*.

(i) Fig. 2(a)&(b): For a single star in the presence of the $\tilde{\Gamma}$ field, the eigenstates of Eq. (6) have a one-to-one correspondence to the lowest energy sector levels of the Hamiltonian (1), with precisely the same degeneracies. This implies that the presence of matter spins in the Hamiltonian (1) does *not* break the parity symmetry among the gauge spins even with a *nonzero* $\tilde{\Gamma}$.

(ii) Fig. 2(c): In the presence of $\tilde{\Gamma}$, the ground state wavefunction of the full Hamiltonian (1) is an equal weight superposition of the eight $P = +1$ configurations and, with smaller but equal weights, the eight $P = -1$ configurations, as should be the case for the exact star operator in the effective Hamiltonian (6). This indicates that, at the single star level, our “molecule” Hamiltonian (1) replicates the quantum dynamics of an exact star operator, even when quantum fluctuations on both the matter and gauge spins are present.

(iii) Fig. 2(d): the ground state energy of a single *plaquette*, as well as the gap to the first excited state, is identical for any fixed configuration of external legs surrounding the plaquette. We have confirmed that this holds for all 128 configurations of external legs, implying that the transverse field $\tilde{\Gamma}$ does not favor any ordering pattern on the lattice. Moreover, the gap to the first excited state is independent of the environment, meaning that the effective plaquette operator generated by $\tilde{\Gamma}$ does not favor any one spin order either.

To our knowledge none of the above quantum features can be attained by constructs elsewhere in the literature. For example, approaches that start with the classical limit $\Gamma = \tilde{\Gamma} = 0$ (e.g., by introducing ancillas [15–22]) suffer from the feature that a finite transverse field will immediately split the ground state degeneracy. In the Supplementary Material, Sec. C, we use a single ancilla in place of the four matter spins (i.e., in the absence of combinatorial symmetry), to illustrate how generic inter-

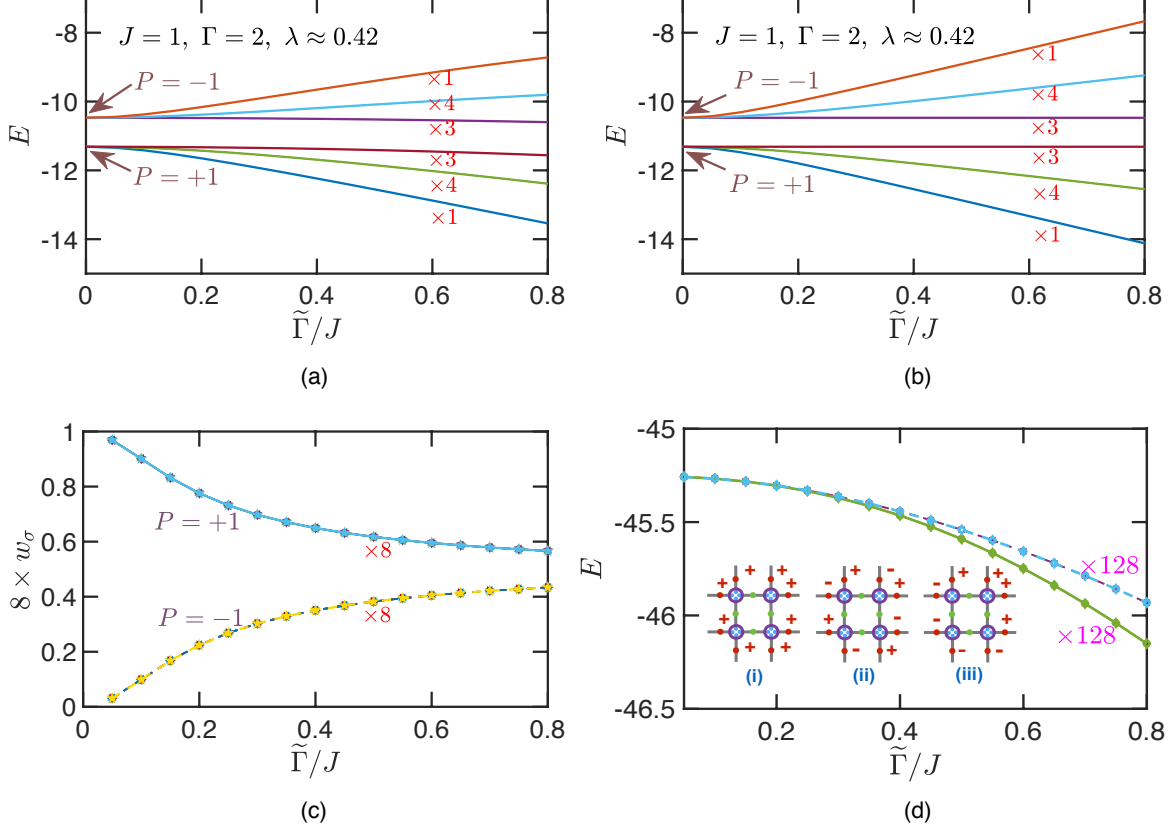


FIG. 2. (a)&(b) Spectrum of a single star as a function of the transverse field $\tilde{\Gamma}$. (a) Lowest energy sector of the full Hamiltonian (1). (b) Complete spectrum of the effective Hamiltonian (6). (c) Weight of the ground state wavefunction of Hamiltonian (1) in the presence of a transverse field $\tilde{\Gamma}$ on each of the eight $P = +1$ and eight $P = -1$ configurations of the star operator, as a function of $\tilde{\Gamma}$. The eight curves in each set fall on top of one another. (d) The ground state and the first excited state energies corresponding to the external leg configurations. The (i)-(iii) insets are examples. For all panels, the degeneracy of each energy level, or the number of curves on top of one another is labeled below the curve by \times . We choose $J = 1$ and $\Gamma = 2$, yielding an excitation gap between the two parity sectors $2\lambda \approx 0.84$.

actions fail to avoid symmetry-breaking ordering even at large Γ .

Embedding in the D-Wave chimera architecture

– Here we show how to embed the two-dimensional surface code in the chimera architecture of the D-Wave machines, using our Hamiltonian (9). (See ref. [31] for details on the D-Wave chimera architecture.)

Because each qubit in a chimera can couple to at most 5 qubits, while our gauge spins must couple to 8, we have to split each gauge spin on the link shared by two vertices into two “twin” spins. The twins are then forced to be equal by a strong ferromagnetic coupling, K , which is set to be the largest coupling in the system [32]. The idea is then to embed each star consisting of 4 matter spins μ_a and 4 gauge spins σ_i into two chimera unit cells of the D-Wave machine, as shown in Fig. 3(a).

We label the 4 gauge spins σ_i by their natural orientations on the lattice: N (North), S (South), W (West) and E (East). Since the 4 matter spins μ_a do not couple

to neighboring sites, their labeling can be chosen arbitrarily and hence not shown explicitly. For each star, we use the intra-chimera couplings within one unit cell to encode the couplings W_{ai} between σ_i and μ_a (depicted in green bonds in Fig. 3). However, in order to couple the gauge spins to neighboring sites both vertically and horizontally, one must make two more copies of the gauge spins using a second unit cell, which can be achieved by strong ferromagnetic couplings that force the spins to be equal (depicted as red bonds in Fig. 3). We exploit that the square lattice is bipartite and distinguish between sublattices A and B so as to properly couple neighboring sites.

Since there are six copies of each gauge spin on the chimera lattice, a transverse field applied to one model gauge spin must flip a total of six device spins. Therefore the effective transverse field $\tilde{\Gamma}$ acting on the gauge spins is of the order $\tilde{\Gamma} \sim \Gamma^6/K^5$. In other words, although the transverse field applied on each physical qubit of the

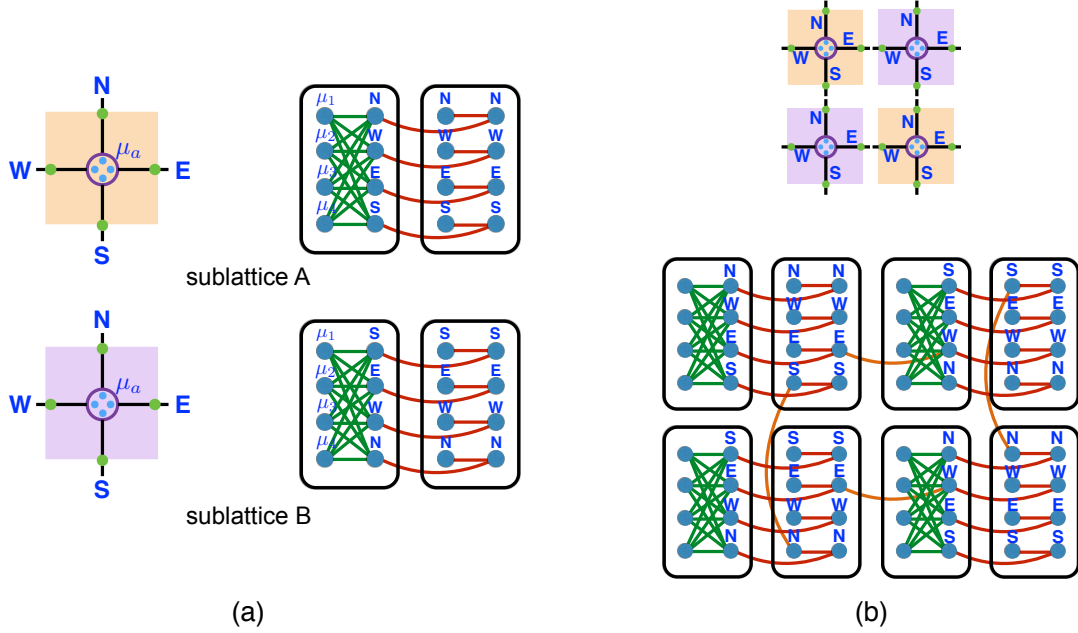


FIG. 3. (a) Embedding of a single vertex (star) of the square lattice into two chimera unit cells, for sublattice A and B , respectively. The intra-chimera couplings depicted in green encode the couplings W_{ai} between gauge spins σ_i and matter spins μ_a . The red bonds are strong ferromagnetic couplings that copy the gauge spins to the second unit cell. (b) Embedding of the surface code model on a 2×2 square lattice into the chimera architecture. The orange bonds denote ferromagnetic couplings between twin spins shared by adjacent sites.

D-Wave machine is uniform, the effective transverse field acting on each gauge spin in the \mathbb{Z}_2 model is suppressed by the ferromagnetic couplings used for copying spins, and is smaller than that acting on the matter spins. The regime where $\tilde{\Gamma}/\lambda$ is small and the Hamiltonian (10) is in the topological phase is thus naturally realized in our embedding. (We remark that one can choose to fix the desired couplings $\tilde{\Gamma}$ and λ and determine the couplings J and Γ from K , via $J = |\lambda \Gamma^3/12|^{1/4}$, see Eq. (8), and $\Gamma \sim |\tilde{\Gamma} K^5|^{1/6}$.)

With the above ingredients, one can readily embed the toric code model on a full square lattice into the chimera architecture. In Fig. 3, we give an explicit embedding of a 2×2 square lattice. Scaling up to bigger system sizes is straightforward. By programming the intra-unit-cell couplings as specified by W_{ai} in Hamiltonian (1), the ferromagnetic couplings for copying spins and the global transverse field, one can realize the \mathbb{Z}_2 gauge theory on currently available D-Wave machines.

To summarize, the above procedure is equivalent to building a \mathbb{Z}_2 quantum gauge model with 256 spins: we use two chimera cells ($2 \times 8 = 16$ qubits) for each star, which contains 2 gauge spins each, totaling the $2048/16 \times 2 = 256$ gauge spins. Within our construction, one can create logical topological qubits by creating holes in the lattice, as is usually done in surface codes [5]. In our scheme, this is simply done by selectively removing couplings in the lattice.

Generalization to other topological states – Frac-

ton topological phases [33–36] (for a review, see Ref. [37]) are novel phases of matter with a robust sub-extensive ground state degeneracy and with excitations that are strictly immobile, or constrained to move within a subdimensional manifold. Apart from theoretical interest such as classifications of phases of matter and formulations in terms of higher-rank gauge theories [38], fracton systems are also believed to hold promise for fault-tolerant quantum computation, as well as robust quantum memory [35]. In spite of the intensive theoretical investigations on fractonic models, experimental realizations directly in terms of spins have barely been discussed [39].

We point out that the building blocks of the \mathbb{Z}_2 gauge theory can also be used to construct 3D models, such as one of the simplest fractonic model, the X-cube [36, 40]. The construction with matter and gauge spins parallels closely that in 2D, and we provide details for the construction of both the 3D toric code and the X-cube model in the Supplementary Materials, Secs. D and E. Embeddings of these 3D gauge-like theories within today’s hardware is possible, in principle, using appropriate graphs. However, such embeddings would be much more efficient in a three-dimensional architecture if or when it becomes available.

Summary and outlook – We have presented a practical way of implementing multi-spin interactions using minimalistic requirements: programmable $\pm J$ ZZ interactions and a uniform X transverse field. These ingredients are available in current quantum hardware, such as in the D-Wave annealers, and hence can be used

to emulate quantum spin liquids and build topological qubits at present-time. The combinatorial symmetry of our blueprint ensures that no local symmetry breaking order can emerge to disturb the liquid states. The work opens up four potentially fruitful directions:

Quantum Memory. Topologically protected qubits can be made by wiring a surface code with holes, i.e., regions where couplings are off. This is probably the most immediate and accessible application of the \mathbb{Z}_2 gauge theory and can be implemented on existing ETS hardware.

Quantum Computation. Due to the relative simplicity of ETS hardware, our approach has the potential to open a path to large scale quantum computation using surface codes, especially if programmable couplings can be adiabatically manipulated [5]. Further, if non-Abelian statistics can be implemented via twists [12–14], then this would be an even more powerful use of the ETS hardware.

Expansion of ETS architectures. What about a

three-dimensional architecture? Is it worth implementing in order to take advantage of the sub-extensive ground state degeneracy of the X-cube model or the improved stability at finite temperature of the 3D toric code [41]?

Playground for Materials Theory. Topologically entangled states [42, 43] have been the focus of theoretical study for some time. It is exciting to think that their features can be probed experimentally in a programmable ETS directly, including testing and optimization of spin geometries, couplings, and statistics. The scheme that we present gives theorists a tool set to design and program multi-body interactions that realize their own spin liquids, with which they can “experiment” themselves by submitting “jobs” to a remote machine.

Acknowledgments – The work by C. C. and Z.-C. Y. is supported by the DOE. The part of the work centered on topological phases of matter is supported by DOE Grant No. DE-FG02-06ER46316; the part of the work centered on quantum information science is supported by Grant No. DE-SC0019275.

-
- [1] IBM, “Infographic: Three types of quantum computing and their applications,” (2015).
 - [2] A. Y. Kitaev, “Fault-tolerant quantum computation by anyons,” *Ann. Phys.* **303**, 2–30 (2003).
 - [3] C. Nayak, S. H. Simon, A. Stern, M. Freedman, and S. Das Sarma, “Non-Abelian anyons and topological quantum computation,” *Rev. Mod. Phys.* **80**, 1083–1159 (2008).
 - [4] E. T. Campbell, B. M. Terhal, and C. Vuillot, “Roads towards fault-tolerant universal quantum computation,” *Nature* **549**, 172 (2017).
 - [5] A. G. Fowler, M. Mariantoni, J. M. Martinis, and A. N. Cleland, “Surface codes: Towards practical large-scale quantum computation,” *Phys. Rev. A* **86**, 032324 (2012).
 - [6] H. Zhang, C.-X. Liu, S. Gazibegovic, D. Xu, J. A. Logan, G. Wang, N. van Loo, J. D. S. Bommer, M. W. A. de Moor, D. Car, R. L. M. Op het Veld, P. J. van Veldhoven, S. Koelling, M. A. Verheijen, M. Pendharkar, D. J. Pennachio, B. Shojaei, J. S. Lee, C. J. Palmstrøm, E. P. A. M. Bakkers, S. D. Sarma, and L. P. Kouwenhoven, “Quantized Majorana conductance,” *Nature* **556**, 74 EP – (2018).
 - [7] K. Boothby, P. Bunyk, J. Raymond, and A. Roy, “Next-generation topology of D-Wave quantum processors,” *D-Wave Technical Report* **22**, 28 (2018).
 - [8] R. Harris, Y. Sato, A. J. Berkley, M. Reis, F. Altomare, M. H. Amin, K. Boothby, P. Bunyk, C. Deng, C. Enderud, S. Huang, E. Hoskinson, M. W. Johnson, E. Ladizinsky, N. Ladizinsky, T. Lanting, R. Li, T. Medina, R. Molavi, R. Neufeld, T. Oh, I. Pavlov, I. Perminov, G. Poulin-Lamarre, C. Rich, A. Smirnov, L. Swenson, N. Tsai, M. Volkmann, J. Whittaker, and J. Yao, “Phase transitions in a programmable quantum spin glass simulator,” *Science* **361**, 162–165 (2018).
 - [9] A. D. King, J. Carrasquilla, J. Raymond, I. Ozfidan, E. Andriyash, A. Berkley, M. Reis, T. Lanting, R. Harris, F. Altomare, K. Boothby, P. I. Bunyk, C. Enderud, A. Fréchet, E. Hoskinson, N. Ladizinsky, T. Oh, G. Poulin-Lamarre, C. Rich, Y. Sato, A. Y. Smirnov, L. J. Swenson, M. H. Volkmann, J. Whittaker, J. Yao, E. Ladizinsky, M. W. Johnson, J. Hilton, and M. H. Amin, “Observation of topological phenomena in a programmable lattice of 1,800 qubits,” *Nature* **560**, 456–460 (2018).
 - [10] F. J. Wegner, “Duality in generalized Ising models and phase transitions without local order parameters,” *J. Math. Phys.* **12**, 2259–2272 (1971).
 - [11] J. B. Kogut, “An introduction to lattice gauge theory and spin systems,” *Rev. Mod. Phys.* **51**, 659–713 (1979).
 - [12] H. Bombin, “Topological order with a twist: Ising anyons from an Abelian model,” *Phys. Rev. Lett.* **105**, 030403 (2010).
 - [13] H. Zheng, A. Dua, and L. Jiang, “Demonstrating non-Abelian statistics of majorana fermions using twist defects,” *Phys. Rev. B* **92**, 245139 (2015).
 - [14] A. Mesaros, Y. B. Kim, and Y. Ran, “Changing topology by topological defects in three-dimensional topologically ordered phases,” *Phys. Rev. B* **88**, 035141 (2013).
 - [15] A. Rocchetto, S. C. Benjamin, and Y. Li, “Stabilizers as a design tool for new forms of the Lechner-Hauke-Zoller annealer,” *Sci. Adv.* **2**, e1601246 (2016).
 - [16] N. Chancellor, S. Zohren, and P. A. Warburton, “Circuit design for multi-body interactions in superconducting quantum annealing systems with applications to a scalable architecture,” *npj Quantum Information* **3**, 21 (2017).

- [17] M. Leib, P. Zoller, and W. Lechner, “A transmon quantum annealer: Decomposing many-body Ising constraints into pair interactions,” *Quantum Science and Technology* **1**, 015008 (2016).
- [18] N. Dattani and N. Chancellor, “Embedding quadratization gadgets on chimera and pegasus graphs,” arXiv preprint arXiv:1901.07676 (2019).
- [19] N. Chancellor, S. Zohren, P. A. Warburton, S. C. Benjamin, and S. Roberts, “A direct mapping of max k-sat and high order parity checks to a chimera graph,” *Scientific reports* **6**, 37107 (2016).
- [20] J. D. Biamonte, “Nonperturbative k -body to two-body commuting conversion Hamiltonians and embedding problem instances into Ising spins,” *Phys. Rev. A* **77**, 052331 (2008).
- [21] Y. b. u. Subaş ı and C. Jarzynski, “Nonperturbative embedding for highly nonlocal Hamiltonians,” *Phys. Rev. A* **94**, 012342 (2016).
- [22] Y. Cao, R. Babbush, J. Biamonte, and S. Kais, “Hamiltonian gadgets with reduced resource requirements,” *Phys. Rev. A* **91**, 012315 (2015).
- [23] S. Bravyi, D. P. DiVincenzo, D. Loss, and B. M. Terhal, “Quantum simulation of many-body Hamiltonians using perturbation theory with bounded-strength interactions,” *Phys. Rev. Lett.* **101**, 070503 (2008).
- [24] S. P. Jordan and E. Farhi, “Perturbative gadgets at arbitrary orders,” *Phys. Rev. A* **77**, 062329 (2008).
- [25] C. G. Brell, S. T. Flammia, S. D. Bartlett, and A. C. Doherty, “Toric codes and quantum doubles from two-body Hamiltonians,” *New Journal of Physics* **13**, 053039 (2011).
- [26] S. A. Ocko and B. Yoshida, “Nonperturbative gadget for topological quantum codes,” *Phys. Rev. Lett.* **107**, 250502 (2011).
- [27] M. Sameti, A. Potočnik, D. E. Browne, A. Wallraff, and M. J. Hartmann, “Superconducting quantum simulator for topological order and the toric code,” *Phys. Rev. A* **95**, 042330 (2017).
- [28] E. Fradkin and L. Susskind, “Order and disorder in gauge systems and magnets,” *Phys. Rev. D* **17**, 2637–2658 (1978).
- [29] E. Fradkin, *Field theories of condensed matter physics* (Cambridge University Press, 2013).
- [30] S. Sachdev, “Lecture notes: \mathbb{Z}_2 gauge theory,” (2018).
- [31] S. Boixo, T. F. Rønnow, S. V. Isakov, Z. Wang, D. Wecker, D. A. Lidar, J. M. Martinis, and M. Troyer, “Evidence for quantum annealing with more than one hundred qubits,” *Nat. Phys.* **10**, 218 (2014).
- [32] C. Chamon, E. R. Mucciolo, A. E. Ruckenstein, and Z.-C. Yang, “Quantum vertex model for reversible classical computing,” *Nat. Commun.* **8**, 15303 (2017).
- [33] C. Chamon, “Quantum glassiness in strongly correlated clean systems: An example of topological overprotection,” *Phys. Rev. Lett.* **94**, 040402 (2005).
- [34] S. Bravyi, B. Leemhuis, and B. M. Terhal, “Topological order in an exactly solvable 3D spin model,” *Annals of Physics* **326**, 839 – 866 (2011).
- [35] J. Haah, “Local stabilizer codes in three dimensions without string logical operators,” *Phys. Rev. A* **83**, 042330 (2011).
- [36] S. Vijay, J. Haah, and L. Fu, “Fracton topological order, generalized lattice gauge theory, and duality,” *Phys. Rev. B* **94**, 235157 (2016).
- [37] R. M. Nandkishore and M. Hermele, “Fractons,” *Annu. Rev. Condens. Matter Phys.* **10**, 295–313 (2019).
- [38] M. Pretko, “Subdimensional particle structure of higher rank $u(1)$ spin liquids,” *Phys. Rev. B* **95**, 115139 (2017).
- [39] Y. You and F. von Oppen, “Majorana quantum Lego, a route towards fracton matter,” arXiv preprint arXiv:1812.06091 (2018).
- [40] C. Castelnovo, C. Chamon, and D. Sherrington, “Quantum mechanical and information theoretic view on classical glass transitions,” *Phys. Rev. B* **81**, 184303 (2010).
- [41] C. Castelnovo and C. Chamon, “Topological order in a three-dimensional toric code at finite temperature,” *Phys. Rev. B* **78**, 155120 (2008).
- [42] X.-G. WEN, “Topological orders and chern-simons theory in strongly correlated quantum liquid,” *International Journal of Modern Physics B* **05**, 1641–1648 (1991), <https://doi.org/10.1142/S0217979291001541>.
- [43] X.-G. Wen, *Quantum Field Theory of Many-body Systems: From the Origin of Sound to an Origin of Light and Electrons (Oxford Graduate Texts)* (Oxford University Press, 2007).

SUPPLEMENTAL MATERIAL

Appendix A: Full spectrum of Hamiltonian Eq. (1)

As discussed in the main text, the Hamiltonian Eq. (1) gives the *same* spectrum of 16 states (corresponding to all the choices of the $\tau_a = \pm 1$) for *all* states with the same parity. Below we list all these eigenvalues, and the corresponding degeneracies (within square brackets), for both parities. Notice that the factors of 8 below account for all the 8 states with a given parity.

• $P = +1$

$$E_{0,+} = -4\sqrt{(2J)^2 + \Gamma^2} \quad [1 \times 8] \quad (\text{A1a})$$

$$E_{1,+} = -2\sqrt{(2J)^2 + \Gamma^2} \quad [4 \times 8] \quad (\text{A1b})$$

$$E_{2,+} = 0 \quad [6 \times 8] \quad (\text{A1c})$$

$$E_{3,+} = +2\sqrt{(2J)^2 + \Gamma^2} \quad [4 \times 8] \quad (\text{A1d})$$

$$E_{4,+} = +4\sqrt{(2J)^2 + \Gamma^2} \quad [1 \times 8] \quad (\text{A1e})$$

• $P = -1$

$$E_{0,-} = -\sqrt{(4J)^2 + \Gamma^2} - 3|\Gamma| \quad [1 \times 8] \quad (\text{A2a})$$

$$E_{1,-} = -\sqrt{(4J)^2 + \Gamma^2} - |\Gamma| \quad [3 \times 8] \quad (\text{A2b})$$

$$E_{2,-} = -\sqrt{(4J)^2 + \Gamma^2} + |\Gamma| \quad [3 \times 8] \quad (\text{A2c})$$

$$E_{3,-} = +\sqrt{(4J)^2 + \Gamma^2} - 3|\Gamma| \quad [1 \times 8] \quad (\text{A2d})$$

$$E_{4,-} = -\sqrt{(4J)^2 + \Gamma^2} + 3|\Gamma| \quad [1 \times 8] \quad (\text{A2e})$$

$$E_{5,-} = +\sqrt{(4J)^2 + \Gamma^2} - |\Gamma| \quad [3 \times 8] \quad (\text{A2f})$$

$$E_{6,-} = +\sqrt{(4J)^2 + \Gamma^2} + |\Gamma| \quad [3 \times 8] \quad (\text{A2g})$$

$$E_{7,-} = +\sqrt{(4J)^2 + \Gamma^2} + 3|\Gamma| \quad [1 \times 8] \quad (\text{A2h})$$

The fact that not only the ground state but all excited states depend on the gauge spin configurations through their parity alone is key to stabilizing the spin liquid state once the stars are placed in the lattice.

Appendix B: Additional detail on numerical results for the \mathbb{Z}_2 gauge theory

Details on the numerical comparison of the effective Hamiltonian with the four-spin interaction and the Hamiltonian with the matter and gauge spins are presented below. The studies focused on clusters containing either a single star or a single plaquette surrounded by a fixed background, in the presence of the transverse field $\tilde{\Gamma}$.

The spectrum of the single star of the effective Hamiltonian Eq. (6) in the presence of a transverse field can be obtained straightforwardly, leading to the following 16 eigenvalues (degeneracies): $\pm\sqrt{\lambda^2 + 16\tilde{\Gamma}^2}$ ($\times 1$), $\pm\sqrt{\lambda^2 + 4\tilde{\Gamma}^2}$ ($\times 4$), $\pm\lambda$ ($\times 3$). The constant shift γ is not shown for simplicity. The lowest eigenstate is an equal superposition of all 8 spin configurations that satisfy $P = +1$ and, with smaller amplitude that varies with increasing $\tilde{\Gamma}$, an equal superposition of all 8 spin configurations that satisfy $P = -1$. Symmetry of the ground state of the molecule is necessary, but not sufficient, for symmetry in the lattice.

Diagonalization of the Hamiltonian Eq. (1) in the presence of the transverse field $\tilde{\Gamma}$ yields states with the exact same degeneracies as those of the effective model on a transverse field presented above. Fig. 2(a) and (b) in the main text present the spectrum for both the effective Hamiltonian with the four-spin interaction and the lowest energy sector for the Hamiltonian with the matter and gauge spins.

To compare the weights of the ground state wavefunction on each of the gauge spin configurations, we take the ground state $|\psi\rangle$ of the Hamiltonian with gauge and matter spins and obtain the reduced density matrix by tracing over the matter spins: $\rho_\sigma = \text{tr}_\mu |\psi\rangle\langle\psi|$, where μ and σ stand for the four matter and gauge spins, respectively. Then

we compute the weight of ρ_σ on each of the sixteen (eight with $P = +1$ and eight with $P = -1$) configurations $|\sigma_\ell\rangle$, $\ell = 1, 2, \dots, 16$:

$$w_{\sigma_\ell} := \text{tr}(\rho_\sigma |\sigma_\ell\rangle\langle\sigma_\ell|). \quad (\text{B1})$$

These weights are displayed in Fig. 2(c). The data show that the ground state wavefunction contains an equal amplitude superposition of the eight $P = +1$ gauge spin configurations and, with smaller weight, the eight $P = -1$ configurations, mirroring exactly the case for the star operator in the effective Hamiltonian with the four-spin interaction. This indicates that, at the single star level, our “molecule” Hamiltonian (1) replicates the quantum dynamics of an exact star operator Eq. (6), even when quantum fluctuations on both the matter and gauge spins are present via the transverse fields.

To further support our claim that the system does not favor any ordered state when placed on the full lattice, we move to the next level of complexity and focus on a single plaquette. Consider a single plaquette surrounded by 8 external links, as depicted in the inset of Fig. 2(d). Suppose we fix the environment as defined by the gauge spins on the external legs. In the absence of the transverse field $\tilde{\Gamma}$, the star constraint of positive parity is satisfied, and there are $2^{8-1} = 128$ external leg configurations compatible with the constraint.

In the case of the effective Hamiltonian (6), there are only two allowed configurations of the free gauge spins satisfying the star constraints: $|\psi_1\rangle$ and $|\psi_2\rangle$, and they are related by the plaquette operator: $|\psi_2\rangle = \prod_{\square} \sigma_i^x |\psi_1\rangle$. In the presence of a transverse field, the ground state and the first excited state of this plaquette must be the symmetric $|\psi_S\rangle$ and antisymmetric $|\psi_A\rangle$ superpositions of $|\psi_1\rangle$ and $|\psi_2\rangle$, respectively; and the energy splitting between these two states is given by the energy scale of the effective plaquette operator.

We find for the “molecule” Hamiltonian Eq. (1) that the same independence on the external leg configuration holds. In Fig. 2(d) shows the ground state and the first excited state energies corresponding to the external leg configurations (i)-(iii) in the inset of Fig. 2(d), respectively. We show in the figure only three out of the 128 combinations of external legs, but we have confirmed that the energies of both the ground state and first excited states are exactly the same for all 128 configurations, within machine precision. This is compelling evidence that the transverse field $\tilde{\Gamma}$ does not energetically favor any specific ordering pattern on the lattice. In other words, the effective plaquette operator generated by the transverse field $\tilde{\Gamma}$ does not favor any one spin order in particular, as it should in a spin liquid.

Appendix C: Example of a naive construction without the symmetries of Eq. (1)

The purpose of this section is to illustrate with a simple example why the matter-gauge spin Hamiltonian must take a particular form. It is necessary to start with the quantum limit of large transverse field Γ , but it is not sufficient. The W -matrix must also obey the symmetries of the effective Hamiltonian at the vertex, or “molecular”, level.

To illustrate this concept we revisit the \mathbb{Z}_2 model of the main text. Suppose that we tried a, seemingly simpler, configuration with only one matter spin, as in Eq. (1),

$$H = -J \left(\sum_{i=1}^4 \sigma_i^z \right) \mu^z - \Gamma \mu^x. \quad (\text{C1})$$

All gauge spins couple to the single matter spin equally, or equivalently we choose a W -matrix with all elements set to unity. This formulation allows us to disentangle the effects of the quantum limit and the form of the interaction. We already know that the classical limit of large J is insufficient to generate a topological state, so once again we start with in the quantum limit of large Γ , but without the symmetries of the interactions in Eq. (1). We will find that once again, order-by-disorder takes over and a subset of the equal parity states are favored. This is more evidence that the Haddamard form of the W -matrix is essential. Nonetheless, it is instructive to see how the construct in Eq. (C1) fails.

We proceed as before and diagonalize the Hamiltonian for a given configuration of the gauge spins. The eigenvalues are given by:

$$E_{\pm} = \pm \left[J^2 \left(\sum_{i=1}^4 \sigma_i^z \right)^2 + \Gamma^2 \right]^{1/2}. \quad (\text{C2})$$

The above expression can be written, for any value of Γ and J , as

$$E_{\pm} = \pm a_0 \pm a_2 \left(\sum_{i=1}^4 \sigma_i^z \right)^2 \pm a_4 \sigma_1^z \sigma_2^z \sigma_3^z \sigma_4^z, \quad (\text{C3})$$

which follows from $(\sigma_i^z)^2 = 1$. a_0 , a_2 and a_4 are constants that depend on J and Γ . In this case we do not have the freedom to cancel the a_2 term so we will have a non-zero pairwise interaction between the gauge spins. To solve for the three a 's we note that there are three conditions, given by the square of the total spin $(\sum_i \sigma_i^z)^2 = 0$ or 16 (parity = +1) and total spin squared = 4 (parity = -1). These conditions imply that:

$$\begin{aligned} a_0 &= \frac{1}{8} \left(-\sqrt{\Gamma^2 + 16J^2} + 5|\Gamma| + 4\sqrt{\Gamma^2 + 4J^2} \right) \\ a_2 &= \frac{1}{16} \left(\sqrt{\Gamma^2 + 16J^2} - |\Gamma| \right) \\ a_4 &= \frac{1}{8} \left(\sqrt{\Gamma^2 + 16J^2} + 3|\Gamma| - 4\sqrt{\Gamma^2 + 4J^2} \right). \end{aligned} \quad (\text{C4})$$

Note that the four-spin term looks like the term that we obtained in the four matter spin model, $a_4 = -\lambda/4$ Eq. (7). Furthermore the leading term of order Γ cancels in both interaction terms a_2 and a_4 .

It is reasonable to conjecture at this point that if we can cancel the a_2 term by introducing an offsetting pairwise interaction between gauge spins then we might recover the \mathbb{Z}_2 theory once again. However we will see that repeating the simple numerical tests of the main text and the previous section of this Supplementary Material immediately reveals that the ground states degeneracy breaks. Consider the modified Hamiltonian of Eq. (C1):

$$H \rightarrow H + a_2 \sum_{i,j} \sigma_i^z \sigma_j^z. \quad (\text{C5})$$

We chose the sign of the a_2 term such that the pairwise interaction cancels in the ground state sector E_- of Eq. (C2). However, the full Hamiltonian encompasses the E_+ energy sector as well, and in this sector the gauge spin two-body interaction *does not* cancel. In fact it is additive. In other words, in spite of the appearance of the required four-body term in the ground state sector (C3), the *full* Hamiltonian (C5) does not obey the four-body symmetry. The pairwise interaction spoils the required feature that the spectrum of (C5) should depend on only the parity of the gauge spins.

Now we turn on the transverse field that couples to the gauge spins. This field mixes the positive and negative sectors E_{\pm} of the full Hamiltonian. And, because we broke the four-body symmetry of the full Hamiltonian by adding the ferromagnetic offset (C5), the degeneracy of the pure four-body term will break, too. This is evident from the following numerical diagonalizations, which follow the same sequence of tests. We check the energy spectrum, projected ground state wavefunction and the energy gap in the plaquette. Comparing Fig. 4(a)-(c) to Fig. 2(a)-(d) shows that all the required degeneracies disappear.

To summarize, we have used a simple example to show that without a Hamiltonian that respects the symmetry of the four-spin interaction (parity) in the whole spectrum, the entire scheme cannot work, even when the low energy sector seems to have the correct symmetry. We believe that this observation also provides a more general insight into why quantum spin liquids are so difficult to find. The required symmetries are quite delicate.

Appendix D: 3D toric code

Following the path that we laid out in two dimensions, we can use the Hamiltonian (1) to generate the toric code in three dimensions, as well. The main difference is that in 3D, we shall put the matter spins at the center of each plaquette (square face) of the cubic lattice, rather than on the vertex, as shown in Fig. 5(a). This will enable us to construct the exact plaquette operator in the σ^z -basis, first. The Hamiltonian for a single plaquette is still given by Eq. (1), for which we have shown that the ground state sector takes the form of the product of four σ^z 's around the plaquette, as in Eq. (6). This yields the exact plaquette term of the 3D toric code. Adding a transverse field $\tilde{\Gamma}$ on the gauge spins and going to the full cubic lattice, we arrive at the lattice Hamiltonian (in the $\tau_a = -1$ sector):

$$H_{\tau=-1} = -\lambda \sum_p \prod_{i \in p} \sigma_i^z - \tilde{\Gamma} \sum_i \sigma_i^x. \quad (\text{D1})$$

When $\tilde{\Gamma}/\lambda$ is small, the leading order term acting within the ground state manifold happens at the sixth order, which involves the product of six σ^x 's on the links emanating from a single vertex. This term is precisely the star operator of the 3D toric code, as shown in Fig. 5(b). Therefore, the same construction can implement the toric code model in both two and three dimensions.

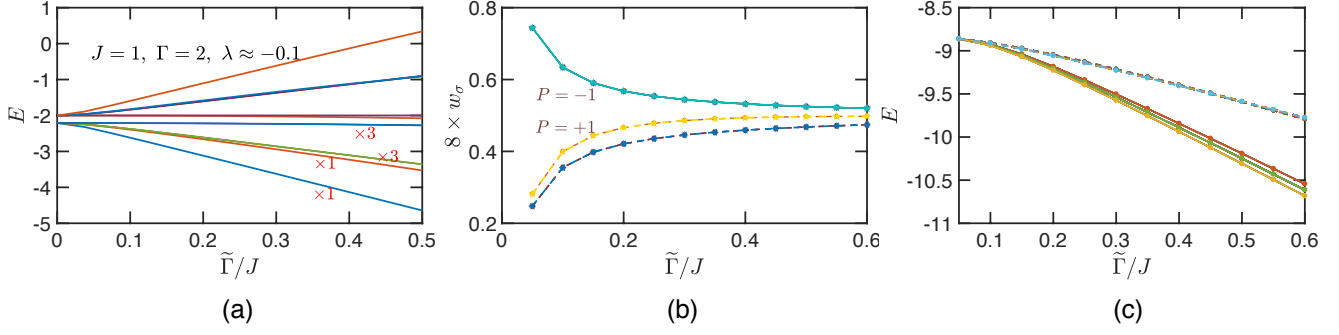


FIG. 4. (a) Energy spectrum of the lowest energy sector of the full Hamiltonian (C5) in the presence of the transverse field $\tilde{\Gamma}$ acting on the gauge spins σ . The degeneracy of each energy level is labeled below the curve. Compare to Figs. 2(a) and (b); the spectrum structure of the one-matter spin Hamiltonian (and its associated degeneracies) is different from both that of the one with four-matter spins and that of the effective model. (b) Weight of the ground state wavefunction of Hamiltonian (C5) in the presence of a transverse field $\tilde{\Gamma}$ on each of the eight $P = +1$ and eight $P = -1$ configurations of the star operator, as a function of $\tilde{\Gamma}$. Compare to Fig. 2(c); the eight $P = +1$ configurations in the one-matter spin Hamiltonian are no longer degenerate (note that in our sign convention the $P = +1$ and $P = -1$ states are reversed). Instead, the eight $P = +1$ states split into two sets: 2 states correspond to the four σ 's having all the same sign, and 6 states correspond to two of the σ 's being positive and two negative. (c) The ground state and the first excited state energies of the Hamiltonian (C5) in the presence of $\tilde{\Gamma}$ corresponding to all 128 possible external leg configurations compatible with the parity constraint. Compare to Fig. 2(d); the ground state energy and the gap to the first excited state is no longer independent of the environment and thus favors an ordered pattern as oppose to a featureless state.

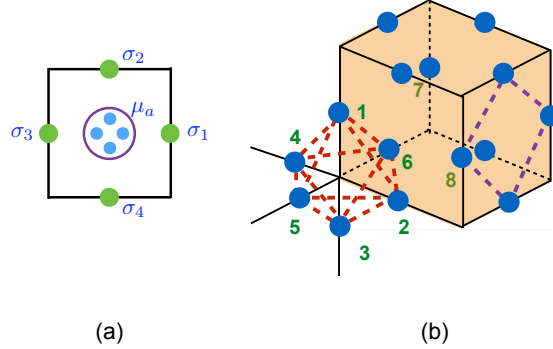


FIG. 5. Construction of three dimensional toric code model. (a) Matter spins are put at the center of each plaquette. (b) The plaquette operator (depicted in purple line), which is a product of four σ^z operators around every face of the cube; and the star operator (depicted in red line), which is a product of six σ^x operators on the links emanating from each vertex.

Appendix E: X-cube model

The X-cube Hamiltonian contains, at each vertex, three star terms associated with three intersecting planes. Fig. 6(a) illustrates the labeling of the 6 spins at the edges of a vertex. The three stars correspond, each, to a product of 4 spins: $B_s^{xy} = \sigma_1^z \sigma_2^z \sigma_4^z \sigma_5^z$, $B_s^{yz} = \sigma_2^z \sigma_3^z \sigma_5^z \sigma_6^z$, and $B_s^{xz} = \sigma_1^z \sigma_3^z \sigma_4^z \sigma_6^z$.

We implement each of the three star operators using the same scheme we used in the toric code. We group the 6 gauge spins in (overlapping) sets of 4 spins, forming four-legged stars. The three groups are (1245), (2356) and (1346), matching the groups in the operators B_s^{xy} , B_s^{yz} and B_s^{xz} above. For each of the different directions, we need a set of 4 matter spins, thus we require 12 matter spins per vertex or site of the cubic lattice. Without the transverse field $\tilde{\Gamma}$ on the 6 gauge spins, the three directions are decoupled, and it thus follows directly from the construction in the

previous section that the $\tau_a = -1$ sector Hamiltonian takes the form

$$\begin{aligned} H_{\tau=-1} &= 3\gamma - \lambda \sigma_1^z \sigma_2^z \sigma_4^z \sigma_5^z - \lambda \sigma_2^z \sigma_3^z \sigma_5^z \sigma_6^z - \lambda \sigma_1^z \sigma_3^z \sigma_4^z \sigma_6^z \\ &= 3\gamma - \lambda (B_s^{xy} + B_s^{yz} + B_s^{xz}) , \end{aligned} \quad (\text{E1})$$

where the coefficients γ and λ are given in terms of J and Γ by Eq. (7). The ground state configuration of each of three star operators B_s^{xy}, B_s^{yz} and B_s^{xz} has positive parity, $P^{xy} = P^{yz} = P^{xz} = +1$, since $\lambda > 0$. (Notice that there is a constraint that the product $P^{xy} P^{yz} P^{xz} = +1$.)

Paralleling the discussion for the 2D \mathbb{Z}_2 gauge theory, there is a regime where $|\Gamma| \rightarrow \infty$ while keeping λ fixed, which opens an infinite gap to the excited sectors with at least one $\tau_a = +1$. The splitting $2|\lambda|$ between the two parity states within the lowest energy sector remains finite. To access this regime we would fix λ and tune $J = |\lambda \Gamma^3 / 12|^{1/4}$ just as in the 2D case.

When $\tilde{\Gamma} = 0$, the spectrum of the gauge-matter Hamiltonian (with six gauge spins and three sets of four matter spins) depends only on the *sum* of the parities $P^{xy} + P^{yz} + P^{xz}$. This is a manifestation of the combinatorial symmetry we identified in the previous section, and this symmetry is again essential to suppressing any interaction that favors any type of order.

So far we have obtained the exact star operators of a single vertex in the X-cube model. Now consider the full cubic lattice in three dimensions where the gauge spins reside on the links and the matter spins reside on the vertices. We apply a transverse field $\tilde{\Gamma}$ to the gauge spins.

First, consider the limit $|\Gamma| \rightarrow \infty$, $J = |\lambda \Gamma^3 / 12|^{1/4}$ with λ fixed (i.e., projecting down to the ground state sector with $\tau = -1$). In this limit, the Hamiltonian on the entire lattice becomes:

$$H_{\tau=-1} = -\lambda \sum_s (B_s^{xy} + B_s^{yz} + B_s^{xz}) - \tilde{\Gamma} \sum_i \sigma_i^x. \quad (\text{E2})$$

In the limit where $\tilde{\Gamma}/\lambda$ is small, the lowest order term in perturbation theory that acts within the ground state subspace is the 12-body interaction around each cube c : $A_c = \prod_{n \in \partial c} \sigma_n^x$, which is the cube operator of the X-cube model. Similar to Hamiltonian (10), we expect that there is a range of small $\tilde{\Gamma}/\lambda$ where the system is in the phase with fractonic topological order. We have thus implemented the full X-cube model on the lattice, using only two-body Ising couplings and a transverse field.

Similar to the implementation of toric code in 2D, we shall now provide numerical evidence indicating that the full Hamiltonian with gauge and matter spins preserves all essential symmetries of the exact star operators in the X-cube model for a wide range of parameters $(\tilde{\Gamma}, \Gamma, J)$. Since there are now three star operators in the X-cube model satisfying the constraint $P^{xy} P^{yz} P^{xz} = +1$, the ground states must have parity $+1$ for all three star operators, or equivalently, $P^{xy} + P^{yz} + P^{xz} = 3$; the excited states are created by flipping the parities of two out of the three stars, i.e. $P^{xy} + P^{yz} + P^{xz} = -1$. In Fig. 6(b)&(c), we plot the eigenenergy spectrum of the ground state sector where $P^{xy} + P^{yz} + P^{xz} = 3$, in the presence of a transverse field $\tilde{\Gamma}$ on the gauge spins. Once again, the levels of the full Hamiltonian [Fig. 6(b)] have a one-to-one correspondence to the levels of the exact star operators [Fig. 6(c)] for nonzero $\tilde{\Gamma}$, with precisely the same degeneracies. While the levels of the excited states are quite complicated to count directly, transitions to the excited states can be captured again by looking at the weight of the ground state wavefunction on every classical configuration, including excited states with $P^{xy} + P^{yz} + P^{xz} = -1$, just like in Fig. 2 for the 2D toric code. This is shown in Fig. 6(d). It is clear that the ground state wavefunction has equal weights on each of the 16 configurations with $P^{xy} + P^{yz} + P^{xz} = 3$ (ground states) and the 48 configurations with $P^{xy} + P^{yz} + P^{xz} = -1$ (excited states), as should be the case for the exact star operators of the X-cube model. While we are unable to perform exact diagonalizations of a single cube surrounded by fixed external legs, as we did in Fig. 2(d) for the toric code in 2D, our numerical results suggest that we indeed replicate a single vertex in the X-cube model even when quantum dynamics is introduced.

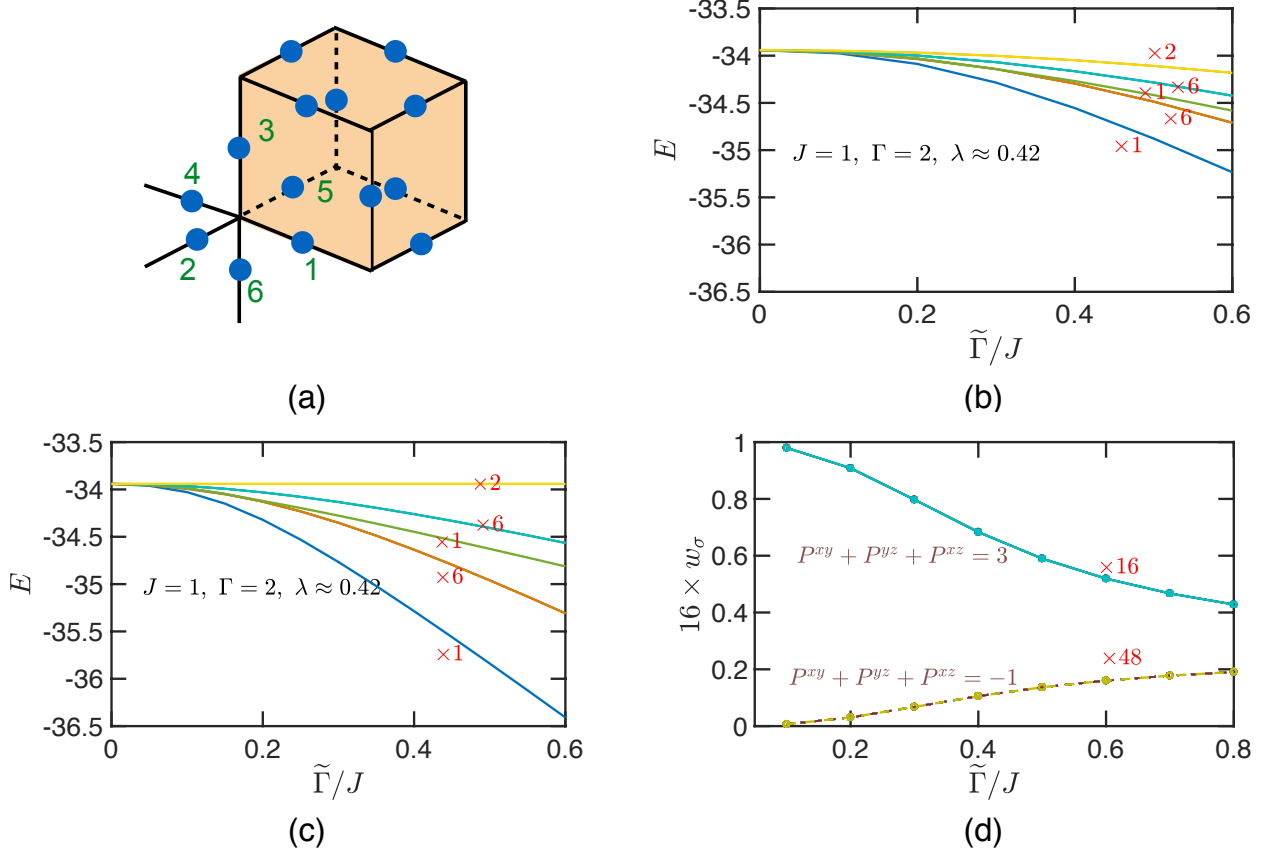


FIG. 6. (a) The X-cube model exhibiting fractonic topological order. The Hamiltonian contains three star terms associated with three intersecting planes: $B_s^{xy} = \sigma_1^z \sigma_2^z \sigma_4^z \sigma_5^z$, $B_s^{yz} = \sigma_2^z \sigma_3^z \sigma_5^z \sigma_6^z$, and $B_s^{xz} = \sigma_1^z \sigma_3^z \sigma_4^z \sigma_6^z$. The cube operator is the product of σ^x around an elementary cube c : $A_c = \prod_{n \in \partial c} \sigma_n^x$. (b)&(c) Eigenenergy spectrum of a single vertex in the X-cube model as a function of the transverse field $\tilde{\Gamma}$ acting on the gauge spins. Only the levels in the ground state sector where all three star operators have parity $P = +1$ are shown. (b) Energy spectrum of the lowest energy sector of the Hamiltonian with gauge and matter spins. (c) Energy spectrum of the effective Hamiltonian (E1). Notice that the eigenstates of the Hamiltonian with gauge and matter spins have precisely the same levels of degeneracy as the effective Hamiltonian with all $\tau_a = -1$. (d) Weight of the ground state wavefunction of the full Hamiltonian in the presence of a transverse field $\tilde{\Gamma}$ on each of the 16 configurations with $P^{xy} + P^{yz} + P^{xz} = 3$ (ground states) and the 48 configurations with $P^{xy} + P^{yz} + P^{xz} = -1$ (excited states) of the X-cube star operators, as a function of $\tilde{\Gamma}$. The curves in each set fall on top of one another, indicating that the ground state in the presence of $\tilde{\Gamma}$ is an equal amplitude superposition of the configurations with $P^{xy} + P^{yz} + P^{xz} = 3$ and those with $P^{xy} + P^{yz} + P^{xz} = -1$, as it should be for the effective Hamiltonian (E1). The degeneracy of each energy level, or the number of curves falling on top of one another is labeled below the curve. The choice of parameters are the same as in Fig. 2.